Monitoring Censored Lifetime Data with a Weighted-Likelihood Scheme

Chi Zhang,[1,2] Fugee Tsung,[2] Dongdong Xiang[1]

[1]*School of Statistics, East China Normal University, Shanghai, China*

[2]*Department of Industrial Engineering & Logistics Management, Hong Kong University of Science and Technology, Hong Kong*

Received 16 June 2015; revised 12 December 2016; accepted 19 December 2016
DOI 10.1002/nav.21724
Published online 19 January 2017 in Wiley Online Library (wileyonlinelibrary.com).

Abstract: Lifetime experiments are common in many research areas and industrial applications. Recently, process monitoring for lifetime observations has received increasing attention. However, some existing methods are inadequate as neither their in control (IC) nor out of control (OC) performance is satisfactory. In addition, the challenges associated with designing robust and flexible control schemes have yet to be fully addressed. To overcome these limitations, this article utilizes a newly developed weighted likelihood ratio test, and proposes a novel monitoring strategy that automatically combines the likelihood of past samples with the exponential weighted sum average scheme. The proposed Censored Observation-based Weighted-Likelihood (COWL) control chart gives desirable IC and OC performances and is robust under various scenarios. In addition, a self-starting control chart is introduced to cope with the problem of insufficient reference samples. Our simulation shows a stronger power in detecting changes in the censored lifetime data using our scheme than using other alternatives. A real industrial example based on the breaking strength of carbon fiber also demonstrates the effectiveness of the proposed method. © 2017 Wiley Periodicals, Inc. Naval Research Logistics 63: 631–646, 2017

Keywords: CUSUM chart; data censoring; EWMA chart; run length distribution; statistical process control; Weibull distribution; weighted likelihood

1. INTRODUCTION

In recent years, there has been an increase in the popularity of lifetime applications. Benefitting from the development in production and experimentation conditions, lifetime applications have become commonplace in medical studies, industrial production lines, as well as reliability areas. For example, in an assembly system, the maximum processing intensity of machine elements must be fully examined before they are accepted for real operation, and only those with a higher intensity tolerance (than a certain threshold) are allowed to be used. In clinical trials, the time course over which desired and adverse effects of a certain drug are likely to occur must be studied comprehensively before that drug can enter the market. Most of these applications share the common feature of incurring a substantial cost once the process parameters shift and the model no longer fits. The assembly system may stop working because of unqualified machine elements, which would easily lead to a high repairing cost. The drug may cause side effects for a much longer period of time when produced from a shifted model. Thus, the production or experiment process must be monitored continuously. With more developed tools for inference, statistical approaches such as statistical process control (SPC) that make use of process information are often preferred in system monitoring/fault diagnosis and have benefited the industrial practice immensely. SPC is a typical monitoring method and has been widely adopted in various engineering applications. Its objective is to detect possible changes in process parameters as soon as they occur, so that remedial actions can be taken without delay (cf., Hawkins and Olwell [9], Woodall and Montgomery [31]). SPC usually consists of Phase I and Phase II. The first phase is the initial establishment of the model and control limits based on historical data, and the second phase is the online monitoring of the process based on the model and control limits from the previous phase.

With respect to the SPC monitoring problem for lifetime applications, several control charts has been proposed under different distributional models, including the exponential, normal, log-normal, or Weibull distribution (see Aslam [2], Baston et al. [3], Khoo and Xie [14], Raza et al. [24], Shafae et al. [25], Steiner and Mackay [27], and Yegulalp [32]). Among these distributions, the Weibull distribution is the most widely investigated due to its flexibility in modeling various lifetime

Correspondence to: Dongdong Xiang (terryxdd@163.com)

models and product failure mechanisms (Chan and Pascual [4], Guo and Wang [6], Lawless [16], Pascual and Li [21], Tobias and Trindade [30]). The Weibull distribution consists of a scale parameter η and a shape parameter β. The type of failure mechanism modeled by the Weibull distribution is determined by the value of the shape parameter β. When $\beta < 1$, the Weibull distribution models early life (failure rate decreases with time). The Weibull distribution models wear out life (failure rate increases with time) when $\beta > 1$, which is also the most common case in real life. When $\beta = 1$, which implies the failure rate is constant with time, the Weibull distribution corresponds to the exponential distribution. In applications, η is more likely to change than β as β is an inherent parameter and often fixed. Thus, most existing works focus on monitoring the changes in scale parameter η by assuming β fixed (Khoo and Xie [12], Tobias and Trindade [25]) or equivalently monitor the distribution mean (Dickinson et al. [5], Steiner and Mackay [28], Zhang and Chen [33]). However, all current studies only consider downward changes in the mean lifetime. In fact, it is also important to monitor increases in η. Although an increase of η is preferred in some situations, a large η usually increases the average cost of the products, especially in laboratory experiments and chemical productions (Lawless [16], Tobias and Trindade [25]). In that sense, it is critical to investigate both upward and downward shift directions when the process is out of control (OC).

To monitor lifetime observations, three challenges are faced. The biggest challenge is the censoring (type-I right censoring) phenomenon, which is quite common in lifetime and many reliability areas. There are several types of censoring (Meeker and Escobar [15]), but we mainly consider type-I right censoring throughout the paper as it is popular in industrial applications (Li and Kong [17]). In a lifetime test, type-I right censoring means one can only observe a predetermined threshold C when the real lifetime value is larger than C. When the lifetime is smaller than C, exact observations can be recorded. The censoring phenomenon greatly increases the difficulties in parameter monitoring as the real lifetimes are only partially observed, and thus the effect of a parameter change may not be fully reflected in the collected data. To overcome this challenge, Dickinson et al. [5], Olteanu [20], Zhang and Chen [33] have proposed various charting schemes and practical suggestions. However, the existing approaches only monitor downward changes in the parameter. We propose a more general approach that tackles both upward and downward shifts in the process.

The second challenge is to develop a control chart with satisfactory performance. In the literature, the performance of a control chart is characterized by the distribution of run length (RL) which is the number of observations needed to signal a change in the monitored sequence. When a process is in control (IC), the IC RL distribution follows a geometric distribution (Hawkins and Olwell [7]), and the IC average run length (ARL) is to be preferred longer. When the process is OC, the OC ARL is preferred to be shorter. Unfortunately, both cannot be simultaneously achieved. As an alternative, most monitoring schemes fix the IC ARL at a desirable level, and evaluate a control chart by comparing their OC ARLs. We show through simulation and a real case verification that our proposed scheme has outstanding performance in terms of both IC and OC scenarios.

The last but not the least contribution is the flexibility of modern control schemes. In lifetime applications, the IC samples are sometimes difficult to collect, and this may lead to uncertainty in IC parameters because of insufficient samples. Here we propose a self-starting charting scheme to address the insufficient IC sample scenario, which can start early and then update the parameter estimates with each new observation.

In this article, motivated by the recent development of the weighted scheme on likelihood (Agostinelli and Markatou [1]), a Censored Observation-based Weighted-Likelihood (COWL) control chart, which integrates the likelihood of past samples, is proposed to monitor the online lifetimes. The merits of this monitoring scheme are five-fold: (i) it focuses on monitoring the more important scale parameter, and it adequately solves the censoring problem; (ii) it provides desirable IC and OC performances; (iii) it captures both increasing and decreasing shifts even under an insufficient IC sample scenario; (iv) although the focus of the paper is on Weibull distributed data, the proposed monitoring scheme can be applied to other parametric families; (v) its implementation is straightforward, and the computational load is light for online monitoring.

The remainder of this article is organized as follows. Section 2 introduces the mathematical formulation of the monitoring problem and some important existing works. Our proposed methodology and some asymptotic properties are described in Section 3. The numerical performance is thoroughly investigated in Section 4. In Section 5, we demonstrates the proposed method using a real-data example from a manufacturing process. The paper concludes with several remarks in Section 6. Some technical details are provided in the Appendix.

2. PROBLEM FORMULATION AND LITERATURE REVIEW

Here, we start from introducing the mathematical formulation of the SPC monitoring problem for lifetime data: As the lifetime observation x follow the Weibull distribution, its probability density function can be written as

$$f(x;\eta,\beta) = \frac{\beta}{\eta}\left(\frac{x}{\eta}\right)^{\beta-1} e^{-(x/\eta)^{\beta}};\ x \geq 0, \{\eta,\beta\} > 0 \quad (1)$$

where η and β are the scale and shape parameters, respectively. As mentioned before, type-I right censoring may occur and we denote the censoring threshold by C. Let y be the censored observation. Obviously, y can be expressed as $y = xI(x \le C) + CI(x > C)$ where $I(\cdot)$ is the indicator function. Also, we can check that and $\rho_C = P(x > C)$ is right the censoring rate. Following the form between y and x, the collected lifetime dataset $\boldsymbol{y}$ can be expressed as $\boldsymbol{y} = \boldsymbol{x}\boldsymbol{I}(\boldsymbol{x} \le C) + C\boldsymbol{I}(\boldsymbol{x} > C)$. It means that the relationship between y and x still holds for each corresponding component of $\boldsymbol{y}$ and $\boldsymbol{x}$. For expositional convenience, we denote the distribution of y as CWeibull(η, β, C)

In this article, our objective is to detect possible change in the scale parameter as early as possible. Under the Phase II scenario, the online single observation y_i is assumed to follow the change-point model

$$y_i \overset{\text{indep}}{\sim} \begin{cases} \text{CWeibull}(\eta_0, \beta_0, C) & \text{for} \quad i = 1, \ldots, \tau, \\ \text{CWeibull}(\eta_1, \beta_0, C) & \text{for} \quad i = \tau + 1, \ldots \end{cases} \tag{2}$$

where $\overset{\text{indep}}{\sim}$ denotes "independently distributed," and τ is the unknown time point when a change occurs. In the field of SPC, the IC parameter η_0 and β_0 are often assumed to be known or can be estimated from an IC dataset, while the OC parameter η_1 remains unknown during the process.

To monitor the censored Weibull lifetime data, Steiner and MacKay [27, 28] first develop the Conditional Expectation Value (CEV) method, and use the arithmetic/geometric mean of the transformed data as the test statistic. Several data transformation schemes are suggested in their work, such as the Weibull CEV approach, the Exponential CEV approach, and the MLE approach. The simulation results reveal a similar detection power among the various schemes.

Later, Zhang and Chen [33] improves the CEV method and develops two one-sided exponential weighted sum average (EWMA) control charts. In this method, the monitoring statistics are

$$T_i^U = \max\left\{(1-\lambda)T_{i-1}^U + \lambda W_i, \omega_0\right\}$$
$$T_i^L = \min\left\{(1-\lambda)T_{i-1}^L + \lambda W_i, \omega_0\right\}$$

where $\omega_0 = 1$. W_i is calculated as

$$W_i = \begin{cases} (y_i/\eta_0)^{\beta_0} & \text{if} \quad y_i < C, \\ (C/\eta_0)^{\beta_0} + 1 & \text{if} \quad y_i = C \end{cases} \tag{3}$$

The above charts (T_i^U and T_i^L) make slight modifications to the exponential CEV method, and the transformed data W_i follows the censored standard exponential distribution. Nevertheless, these charts perform well only when group data (i.e., multiple observations at each time point) can be collected. In addition, they sometimes cannot reach a prespecified IC ARL (also called discreteness in RL distribution), and thus their IC performances are consequently diminished.

Dickinson et al. [5] proposes the CUSUM chart for monitoring censored reliability/lifetime data. It is effective for both single and group data. Under the single observation scenario, the charting statistics of the CUSUM chart are

$$C_i^+ = \max[0, C_{i-1}^+ + y_i - k_i]$$
$$C_i^- = \min[0, C_{i-1}^- + y_i - k_i]$$

where y_i is the single observation and $k_i = -\frac{r_i \beta_0 \log\left(\frac{1}{1-d}\right)}{\left(1-\left(\frac{1}{1-d}\right)^{\beta_0}\right)}$. The parameter d taking values in (0, 1) is the relative shift size and it means the scale parameter shifts from η_0 to $(1-d)\eta_0$. r_i denotes whether the observation is censored ($r_i = 1$ when the observation is not censored, otherwise $r_i = 0$). The CUSUM chart presents several benefits, but the discreteness in its RL distribution still exists in the CUSUM scheme. In addition, this CUSUM chart only considers the decreasing shift in η (positive d), and it neglects the shift in the increasing side.

3. PROPOSED CONTROL CHART

In this section, we will at first introduce the observed likelihood. Based on that, our proposed control chart with exponential weight is constructed. The guidelines on its design parameters are also provided. At last, we develop a self-starting chart under the case when the historical data are insufficient.

3.1. Observed Likelihood

In existing monitoring methods such as the CEV method, the transformation scheme does not fully utilize the information of the censored observations. In statistical analysis, when the distribution of the observed data is provided, the likelihood ratio test (LRT) is popularly applied and the test is proved asymptotically optimal under some conditions. Thus, it is necessary to derive the likelihood of the Weibull lifetimes. However, because of the censoring phenomenon, the likelihood of the censored observations is different from the traditional likelihood. Kim and Shao [15] (also see Meeker and Escobar [18]) introduced a form of observed likelihood for such data, which is

$$L_{\text{obs}}(\boldsymbol{y}; \boldsymbol{\theta}) = \prod_{\delta_i = 1} [f(y_i; \boldsymbol{\theta}) \pi(y_i; \boldsymbol{\theta})] \times \prod_{\delta_i = 0} \left[\int_{y_i}^{+\infty} f(x; \boldsymbol{\theta}) \{1 - \pi(x; \boldsymbol{\theta})\} \, dx \right]$$

where $\boldsymbol{\theta}$ and $\boldsymbol{y}$ are the parameter and dataset (may be exact or censored), respectively. $f(\cdot)$ denotes the probability density function for exact observations. δ_i equals 1 or 0 indicating

whether the corresponding observation is censored. $\pi(\cdot)$ is the conditional probability that $\pi(y_i;\boldsymbol{\theta}) = P(\delta_i = 1|y_i;\boldsymbol{\theta})$. For Weibull lifetimes, assume that x_i is the true lifetime data and y_i is the observation, $\pi(y_i;\boldsymbol{\theta}) = \delta_i = 1$ when the observation is not censored, otherwise $\pi(y;\boldsymbol{\theta}) = \delta_i = 0$. Thus, the observed log-likelihood for censored data can be written as

$$\begin{aligned} l_{\text{obs}}(\mathbf{y};\eta,\beta) &= \sum_{i=1}^{n}\delta_i f(y_i;\eta,\beta) + \sum_{i=1}^{n}(1-\delta_i)P(x_i > C) \\ &= \sum_{i=1}^{n}\delta_i f(y_i;\eta,\beta) + \sum_{i=1}^{n}(1-\delta_i)\rho_c \end{aligned} \tag{4}$$

Unlike the other data transformation schemes, this likelihood formula extracts information from both exact observations and censored observations simultaneously, and thus more statistical analysis tools can be applied. Dickinson et al. [5] provided a similar equation to derive the CUSUM statistic. In this article, this observed likelihood is extended and the new use of LRT is demonstrated to monitor lifetime observations.

3.2. Censored Observation-Based Weighted-Likelihood Control Chart

To solve the monitoring problem formulated in Eq. (2), the LRT statistic for a single observation can be easily constructed when the observed likelihood is achieved. To realize sequential detection, motivated by Agostinelli and Markatou [1], Qiu et al. [22], Zhou et al. [34] and recalling the popular exponential weighted sum average (EWMA) scheme in quality control, we consider the weighted sum of log-likelihoods (denoted as $wl_{\text{obs}}(\eta,\beta;\mathbf{y},\lambda)$) by the following expression

$$wl_{\text{obs}}(\eta,\beta;\mathbf{y},\lambda) = \sum_{j=0}^{t} w_{j,\lambda} l_{\text{obs}}(\eta,\beta;y_j) \tag{5}$$

where λ is the EWMA smoothing parameter ranging from $(0,1]$, $l_{\text{obs}}(\eta,\beta;y_j)$ is the observed log-likelihood of each observation and $w_{j,\lambda} = \lambda(1-\lambda)^{t-j}$ is exactly the weight of the EWMA strategy. When $j=0$, the mean of the censored Weibull distribution and the noncensoring rate are selected as the "observation" $\{y_0,\delta_0\}$, respectively. By applying the weighted-likelihood strategy, the information of past observations is integrated so that the shift trend can be detected quickly when the process is OC.

Similar to the traditional MLE procedure, the weighted sum of log-likelihoods are maximized to determine the estimated parameters. Following the notations in Eq. (1), when n online observations $\boldsymbol{y} = [y_1, y_2, \ldots, y_n]$ are provided, the estimated value of the scale parameter $\hat{\eta}_n$ has a closed form expression

$$\hat{\eta}_n = \underset{\eta}{\text{argmax}}\, wl_{\text{obs}}(\eta;\mathbf{y},\beta_0,\lambda)$$

$$= \begin{cases} \left(\frac{\sum_{j=0}^{n}\omega_{j,\lambda}[\delta_j y_j^{\beta_0} + (1-\delta_j)C^{\beta_0}]}{\sum_{j=0}^{n}\omega_{j,\lambda}\delta_j}\right)^{\frac{1}{\beta_0}} & \text{if} \quad \sum_{j=0}^{n}\omega_{j,\lambda}\delta_j \neq 0, \\ \eta_0 & \text{if} \quad \sum_{j=0}^{n}\omega_{j,\lambda}\delta_j = 0 \end{cases} \tag{6}$$

Then, we can build the weighted LRT and the test statistic is

$$\begin{aligned} T_{\{\eta\},n} &= wl_{\text{obs}}(\hat{\eta}_n;\mathbf{y},\beta_0,\lambda) - wl_{\text{obs}}(\eta_0;\mathbf{y},\beta_0,\lambda) \\ &= \sum_{j=0}^{n}\omega_{j,\lambda}\delta_j \log \frac{\sum_{j=0}^{n}\omega_{j,\lambda}\delta_j}{\sum_{j=0}^{n}\omega_{j,\lambda}\left[\delta_j\left(\frac{y_j}{\eta_0}\right)^{\beta_0} + (1-\delta_j)\left(\frac{C}{\eta_0}\right)^{\beta_0}\right]} \\ &\quad - \sum_{j=0}^{n}\omega_{j,\lambda}\delta_j + \sum_{j=0}^{n}\omega_{j,\lambda}\left[\delta_j\left(\frac{y_j}{\eta_0}\right)^{\beta_0} + (1-\delta_j)\left(\frac{C}{\eta_0}\right)^{\beta_0}\right] \\ &= Q_n \log Q_n - Q_n \log Z_n - Q_n + Z_n \end{aligned} \tag{7}$$

where $Q_n = \sum_{j=0}^{n}\omega_{j,\lambda}\delta_j$, $Z_n = \sum_{j=0}^{n}\omega_{j,\lambda}[\delta_j\left(\frac{y_j}{\eta_0}\right)^{\beta_0} + (1-\delta_j)\left(\frac{C}{\eta_0}\right)^{\beta_0}]$. In fact, Q_n acts as the weighted sum of censored counts while Z_n is the sum of transformed observations. To be specific, when the observation y_i comes from the censored Weibull distribution with parameters $\{\eta_0,\beta_0,C\}$, the statistic $\left(\frac{y}{\eta_0}\right)^{\beta_0}$ follows the censored standard exponential distribution. This reminds us of the exponential CEV method proposed by Steiner and Mackay [27], in which a similar transformation scheme is applied. However, the exponential CEV method replaces the original observation with the expectation of the censored data, and constructs the monitoring statistic by taking the arithmetic mean. In this article, the monitoring statistic $T_{\{\eta\},n}$ is derived from the weighted LRT test, and it is related to both the weighted sum of censored counts and the transformed observations.

To construct the control chart for online monitoring, the derived statistic $T_{\eta,n}$ is used as the charting statistic. The control chart is referred to as the COWL chart, and it triggers an alarm when $T_{\{\eta\},n}$ exceeds a certain control limit L. The initial value $(y_0,\ \delta_0)$ of the monitoring sequence can be seen as a pseudosample from the censored Weibull population, and our method is robust with different initial values. In this article, The value of $(y_0,\ \delta_0)$ is suggested to be $(\eta_0\Gamma^*(1+\frac{1}{\beta_0},C) + \rho_C,\ 1-\rho_C)$, where $\Gamma^*(,x)$ denotes the incomplete gamma function integrated from 0 to x, and $\eta_0\Gamma^*(1+\frac{1}{\beta_0},C) + \rho_C$ is actually the mean of the censored Weibull data.

Despite the difficulties that the censoring phenomenon brings, our method is quite intuitive. Recalling Z_n in Eq. (7), it degenerates to the traditional EWMA statistic when censoring does not exist, where $\delta_i = 1$ for all i, and consequently $T_{\{\eta\},n}$ can be rewritten as a converted EWMA sequence. Thus, our method could be treated as an extension of the traditional

EWMA scheme that extracts more information under censoring. To reveal more properties of the monitoring statistic, the next Proposition 1 is obtained, and its proof is provided in the Appendix.

PROPOSITION 1: Suppose the observations $y_1, y_2, \ldots, y_n$ come from the IC process, as $\lambda n \to \infty$ and $\lambda \to 0$, we have the following result

$$\frac{A}{\sum_{j=1}^{n} \omega_{j,\lambda}^2 B} T_{\{\eta\},n} \xrightarrow{d} \chi^2(1)$$

Here A, B are some constants related to the IC parameters $\{\eta_0, \beta_0\}$ and the censoring threshold C. Their expressions can be found in the Appendix. This asymptotic result ensures the effectiveness of our proposed method. We see that when n is large, $\sum_{j=1}^{n} \omega_{j,\lambda}^2$ gradually converges, and the asymptotic marginal distribution of the charting statistic can be obtained. Moreover, this proposition also presents us with some interesting statistical insights; that is, first, the asymptotic chi-square property of LRT holds even if the sample likelihoods are given different weights; second, the asymptotic distribution actually does not depend on the nature of Weibull distribution, thus the asymptotic results should also maintain for other parametric families. Therefore, the weighted LRT scheme can be developed for other scenarios and is quite appealing indeed.

Extension to Two-Parameter Monitoring: Although the shape parameter is less likely to change and we focus on monitoring the scale parameter in this article, our control chart is also competent at monitoring the two parameters simultaneously after simple extensions. The detection procedure is similar except β is no longer a constant, and the test statistic is formulated as

$$\begin{aligned} T_{\{\eta,\beta\},n} &= wl_{\text{obs}}(\hat{\eta}_n, \hat{\beta}_n; \boldsymbol{y}, \lambda) - wl_{\text{obs}}(\eta_0, \beta_0; \boldsymbol{y}, \lambda) \\ &= \sum_{j=0}^{n} \omega_{j,\lambda} \Bigg(\delta_j \Bigg[-\hat{\beta}_n \log \hat{\eta}_n + \log \hat{\beta}_n \\ &\quad + (\hat{\beta}_n - 1) \log y_j - \left(\frac{y_j}{\hat{\eta}_n} \right)^{\hat{\beta}_n} \Bigg] \Bigg) \\ &\quad - \sum_{j=0}^{n} \omega_{j,\lambda} \Bigg(\delta_j \Bigg[-\beta_0 \log \eta_0 + \log \beta_0 \\ &\quad + (\beta_0 - 1) \log y_j - \left(\frac{y_j}{\eta_0} \right)^{\beta_0} \Bigg] \Bigg) \\ &\quad + \sum_{j=0}^{n} \omega_{j,\lambda} (1 - \delta_j) \left(\frac{C}{\eta_0} \right)^{\beta_0} \\ &\quad - \sum_{j=0}^{n} \omega_{j,\lambda} (1 - \delta_j) \left(\frac{C}{\hat{\eta}_n} \right)^{\hat{\beta}_n} \end{aligned} \tag{8}$$

where $\left\{ \hat{\eta}_n, \hat{\beta}_n \right\} = \text{argmax}_{\eta,\beta} wl_{\text{obs}}(\eta, \beta; \boldsymbol{y}, \lambda)$ is also from the maximum weighted likelihood estimation. In simultaneous monitoring, nevertheless, there is no closed form expression for estimated parameters $\left\{ \hat{\eta}_n, \hat{\beta}_n \right\}$. Thus, numerical methods are required to find their solutions. Similar to the single-parameter scenario, the control chart sounds an alarm when $T_{\{\eta,\beta\},n}$ exceeds the control limit L.

Choice of the EWMA weight parameter λ: The EWMA smoothing parameter λ is a very important parameter, and an appropriate λ can well benefit the performance of the control chart. In our scheme, λ is chosen to balance the information from the past samples and that from the current observation. Combining some general suggestions for designing EWMA control charts (Stoumbos and Sullivan [29], Zhou et al. [34], Zou and Tsung [36]), we recommend choosing λ between $[0.02, 0.1]$. Noticing that the IC RL distribution is sometimes discrete in previous methods, however, the simulation studies show that almost every IC ARL could be achieved with our chart when λ is within this range. Also, we note the conclusion that smaller λ leads to quicker detection for small shifts still holds in the COWL chart. Although the censoring rate may influence the value of optimal λ, the range $[0.02, 0.1]$ is generally appropriate for the proposed monitoring scheme.

Selecting the control limit: The control limit is a very important parameter to select in our method. And this is often implemented by Monte Carlo simulation. For a prefixed limit L, a Weibull sample is simulated and the charting statistic $T_{\eta,1}$ is calculated. If $T_{\eta,1}$ is smaller than L, another Weibull sample is simulated and the charting statistic is updated as $T_{\eta,2}$. This process is performed repeated until the charting statistic $T_{\eta,k}$ (assume at the kth step) goes beyond the control limit, and the RL k is recorded. The whole running procedure is performed many times (50,000 times in our later simulation study), and finally the IC ARL for the control limit L is obtained. If the obtained IC ARL is smaller than the prefixed one, the control limit is adjusted to be larger, otherwise it is adjusted to be smaller until the obtained IC ARL equals to the prefixed one.

Diagnostic method: In the practice of quality control, an imperative task after the control chart signals is to find the location of the change point at which the monitoring system becomes OC. The diagnostic procedure is particularly important for lifetime studies as the contaminated samples may influence the subsequent experiments. To this end, the traditional idea of general LRT is applied. Recalling that the unknown change point τ divides the collected samples into pre-τ samples (IC samples, $\boldsymbol{y}_{[1,\tau-1]}$) and post-$\tau$ samples (OC samples, $\boldsymbol{y}_{[\tau,\infty]}$), and the likelihood of the whole samples changes as the location of τ varies. Therefore, when an OC signal appears at time point n, the estimated change point is the time when the likelihood ratio between the changed scenario and the unchanged scenario is maximized, that is

$$\begin{aligned}\hat{\tau} &= \arg\max_{t\in[1,2,\ldots,n-1]} \sum_{i=1}^{t} l_{\text{obs}}(y_i;\eta_0,\beta_0) \\ &\quad + \sum_{j=t+1}^{n} l_{\text{obs}}(y_j;\hat{\eta},\beta_0) - \sum_{k=1}^{n} l_{\text{obs}}(y_k;\eta_0,\beta_0) \\ &= \arg\max_{t\in[1,2,\ldots,n-1]} \sum_{j=t+1}^{n} l_{\text{obs}}(y_j;\hat{\eta},\beta_0) - \sum_{k=t+1}^{n} l_{\text{obs}}(y_k;\eta_0,\beta_0)\end{aligned} \tag{9}$$

where $\hat{\eta} = \text{argmax}_\eta \sum_{j=t+1}^{n} l_{\text{obs}}(y_j;\eta,\beta_0)$ and is estimated from the post-τ samples. This estimation formula is consistent with the idea in Joseph and Thomas [13], where the estimation accuracy is proved to be quite favorable.

3.3. A Self-Starting Version of the COWL Chart

In the COWL control chart, it is assumed that the IC parameters $\{\eta_0,\beta_0\}$ can be accurately estimated from the Phase I procedure, in which a large number of reference samples is needed. However, this may not always be true. Considering the high cost of conducting lifetime experiments, the number of reference samples is always limited. As Jenson et al. [11] and Jones et al. [12] point out, there would be much uncertainty in the estimated parameters if there are not enough reference samples, and it may severely affect the IC RL performance as well as the detection power of the proposed chart. To avoid this limited sample size issue, we introduce the self-starting strategy.

Motivated by Qiu and Zou [23], the online monitored samples can be made use of when the number of reference samples is limited. We denote m reference samples by $\boldsymbol{y}_{\text{ref}} = [y_{-m+1},\ldots,y_0]$ and assume the online monitoring process (starting from $t=1$) does not trigger an OC signal at time $n-1$. The self-starting strategy basically uses the pooled samples $[y_{-m+1},\ldots,y_0,y_1,\ldots,y_{n-1}]$ to update the IC parameters. That is, the IC parameter η is recursively updated by

$$\begin{aligned}\hat{\eta}_n &= \underset{\eta}{\text{argmax}}\, wl_{\text{obs}}(\eta;\boldsymbol{y},\beta_0,\lambda) \\ &= \begin{cases} \left(\frac{\sum_{j=-m+1}^{n-1}[\delta_j y_j^{\beta_0}+(1-\delta_j)C^{\beta_0}]}{\sum_{j=-m+1}^{n-1}\delta_j}\right)^{\frac{1}{\beta_0}} & \text{if} \quad \sum_{j=-m+1}^{n-1}\delta_j \neq 0, \\ \eta_0 & \text{if} \quad \sum_{j=-m+1}^{n-1}\delta_j = 0 \end{cases}\end{aligned} \tag{10}$$

Then the charting statistic is the difference in weighted log-likelihoods as before, that is,

$$T^{SS}_{\{\eta\},n} = wl_{\text{obs}}(\hat{\eta}_n,\beta_0;\boldsymbol{y},\lambda) - wl_{\text{obs}}(\hat{\eta}_0^{n-1},\beta_0;\boldsymbol{y},\lambda)$$

where $\hat{\eta}_n$ comes from Eq. (6), and $\hat{\eta}_0^{t-1}$ is the updated parameter calculated from pooled samples at time $n-1$. The derivation for $T^{SS}_{\{\eta\},n}$ is similar to the previous nonself-starting case, and we name this self-starting version of our control chart the SS-COWL control chart.

The properties of the SS-COWL control chart will be investigated later under different circumstances. To better understand the SS-COWL chart, some technical issues are discussed here. It is noted that as the parameter $\hat{\eta}_0^n$ is updated at every time point, the computational load becomes inevitably heavy when n is large. However, there is no need to keep updating the estimated parameters once enough IC samples are collected. According to the property of MLE, the estimated value $\hat{\eta}_0^n$ is indeed close enough to the true parameters η_0 when enough IC samples are collected. Thus, for a large value n_0, we can simply use $\hat{\eta}_0^{n_0}$ as the true parameter for future monitoring. Besides, stopping the parameters update at an appropriate time can help to reduce the "masking-effect" as well (Hawkins [8]). The estimated parameter $\hat{\eta}_0^n$ may be easily contaminated by the later OC samples if the parameters are updated each time, which would sharply reduce the detection power.

4. SIMULATION STUDIES

In this section, the numerical realization of the proposed COWL control chart is investigated, from the perspective of both IC and OC performance. We then compare our chart with two alternative methods: the EWMA-CEV method (Zhang and Chen [33]) and the CUSUM chart (Dickinson et al. [5], Olteanu [20]). In Section 4.1, we compare the IC performance of the selected charts. In Section 4.2, we compare their OC performances. In Section 4.3, we discuss the property of the self-starting control chart. The single observation case is studied in the simulation, and this setting is applied in both CUSUM and COWL charts. As the RL distribution of the EWMA-CEV method becomes discrete under the individual observation setting and the chart cannot reach a prefixed IC ARL, the group data case is utilized in this method to smooth the incontinuity and the group size is fixed at 3. The IC ARL is fixed at 370 throughout the simulation except in several scenarios. The Fortran code for implementing the proposed method is available from the authors upon request.

In Section 4.1 and 4.2, the aforementioned control charts are investigated under various circumstances. Considering the significant impact brought by the censoring phenomenon, data with a low censoring rate $\rho_C = 0.1$, a medium censoring rate $\rho_C = 0.4$ and a high censoring rate $\rho_C = 0.7$ are all discussed. Another factor that may influence the performance of the control chart is the shape of the Weibull data. Particularly, the shape of the probability density function of the Weibull distribution is unimodal when β is larger than 1, while it is degressive when β is smaller than 1. We investigate the Weibull data with the different shape parameters including

Table 1. IC ARL comparison when $\beta = 1$ ($\eta_0 = 1$).

Censoring rate	Method	L	ARL_0	SDRL	Q (.10)	Median	Q (.90)	FAR
	EWMA-CEV	0.882/1.11	370	331	75	270	798	0.0169
$\rho_C = 0.7$	CUSUM	−3.938/ 8.563	370	359	51	260	832	0.066
	COWL	80.625	370	370	39	256	854	0.0953
	EWMA-CEV	0.841/1.162	373	335	75	273	810	0.0179
$\rho_C = 0.4$	CUSUM	−4.410/10.125	370	367	43	259	848	0.0853
	COWL	81.475	369	370	38	257	852	0.0953
	EWMA-CEV	0.814/1.206	370	328	75	270	798	0.0194
$\rho_C = 0.1$	CUSUM	−4.554/10.836	369	371	38	255	850	0.0965
	COWL	79.913	370	370	39	257	851	0.095

Table 2. IC ARL comparison when $\beta = 1.5$ ($\eta_0 = 2$).

Censoring rate	Method	L	ARL_0	SDRL	Q (.10)	Median	Q (.90)	FAR
	EWMA-CEV	0.883/1.11	370	332	75	270	795	0.0168
$\rho_C = 0.7$	CUSUM	−2.511/7.5	369	359	45	258	840	0.0794
	COWL	80.625	370	370	39	257	855	0.0942
	EWMA-CEV	0.842/1.162	370	331	75	267	798	0.0182
$\rho_C = 0.4$	CUSUM	−2.711/8.656	369	371	37	254	858	0.0981
	COWL	81.475	371	370	39	258	853	0.0935
	EWMA-CEV	0.814/1.207	371	331	75	270	807	0.0178
$\rho_C = 0.1$	CUSUM	−2.75/9.094	368	369	36	255	852	0.101
	COWL	80.625	370	370	39	257	849	0.0944

$\beta = \frac{1}{3}(< 1)$, $\beta = 1$ and $\beta = 1.5(> 1)$ in the simulation (note that the Weibull distribution becomes the exponential distribution when $\beta = 1$). The reference shift size in the CUSUM chart is d, and both increasing and decreasing shifts are considered. The ARL values are obtained from 50,000 replicated steady-state simulations.

4.1. In Control Performance

We first compare the IC performance of our proposed COWL, the EWMA-CEV, and the CUSUM chart. As mentioned in Mei [19], simply using the ARL to describe the behavior of control charts may not be informative enough, especially for an IC performance study. Instead, we study the IC RL distribution. Suggested by Shen et al. [26] and Zhou et al. [34], several indices of the IC RL distribution (IC indices) are selected, including the distribution's percentiles, standard deviation of the run length (SDRL), and also the false alarm rate for the first t observations, $\Pr(T \leq t)$, where T is the stopping time of a monitoring sequence. As mentioned beforehand, the IC RL distribution is satisfactory when it follows the geometric distribution, or the distribution indices are close to those of the geometric one. Here we use L, $Q(.10)$, median, $Q(.90)$ and FAR to denote the control limit, 10th percentile, 50th percentile, 90th percentile and false alarm rate for the first 37 observations $\Pr(T \leq 37)$, respectively. Under the real geometric distribution, when ARL_0 equals to 370, the quantity of the SDRL, $Q(.10)$, median, $Q(.90)$, and FAR are about 370, 37, 257, 851, and 0.0953, respectively. The parameter d in the CUSUM chart is fixed at 50%, and the two-sided shift parameters equal to $\eta_1 = (1+d)\eta_0$, $\eta_2 = (1-d)\eta_0$. In both EWMA control charts, the weight parameter $\lambda = 0.05$ for consistency (Stoumbos and Sullivan [29], Zhou et al. [34], Zou and Tsung [36]). The approaches for selecting the control limit follow our suggestions in Section 3.

The results of the IC performance study are summarized in Tables 1–3. The IC parameter η_0 in the three tables are 1, 2, and 0.5, and the corresponding shape parameter β equals to 1, 1.5, and $\frac{1}{3}$. From the result in Table 1, we can see that both the EWMA-CEV chart and COWL control chart perform stably under various censoring rates, and the COWL chart provides a closer IC RL distribution to the geometric distribution. For the CUSUM chart, its IC performance is influenced by the censoring rate ρ_C. The IC indices are close to the target ones when ρ_C equals 0.1. However, as the censoring rate increases, say to $\rho_C = 0.7$, the indices deviate significantly and the IC performance of the CUSUM chart deteriorates. Another issue that deserves more discussion is SDRL. In Table 1, it can be seen that both the EWMA-CEV method and the CUSUM chart have a smaller SDRL than ARL_0 under IC scenario when ρ_C is large, which seems to be a benefit. However, combining the values of FAR, we find that the small SDRL of the EWMA-CEV method may be due to the very small proportion of short-run false alarms (a very small FAR value). Thus, the chart could fail to detect shifts quickly (Zhou et al. [34]). One reason to explain the low value

Table 3. IC ARL comparison when $\beta = \frac{1}{3}$ ($\eta_0 = 0.5$).

Censoring rate	Method	L	ARL_0	SDRL	Q (.10)	Median	Q (.90)	FAR
	EWMA-CEV	0.882/1.110	372	332	75	270	801	0.0181
$\rho_C = 0.7$	CUSUM	−8.438/11.5	372	317	84	280	778	0.0185
	COWL	80.625	370	370	38	256	853	0.0963
	EWMA-CEV	0.841/1.162	374	339	75	270	813	0.017
$\rho_C = 0.4$	CUSUM	−10.313/14.75	374	333	73	275	805	0.0269
	COWL	81.475	369	370	38	257	851	0.0956
	EWMA-CEV	0.814/1.207	369	328	75	270	792	0.0187
$\rho_C = 0.1$	CUSUM	−11.34/16.61	374	343	66	270	818	0.0361
	COWL	79.91	371	371	39	257	851	0.0944

Table 4. Sensitivity analysis on control limit.

Method	L	Orig. Scenario $\rho_C = 0.7, \beta = 1$	Scenario(I) $\rho_C = 0.4, \beta = 1$	Scenario(II) $\rho_C = 0.1, \beta = 1$	Scenario(III) $\rho_C = 0.7, \beta = \frac{1}{3}$	Scenario(IV) $\rho_C = 0.7, \beta = 1.5$
EWMA-CEV	0.881/1.11	370 (331)	101 (78.1)	60.3 (43.3)	370 (329)	370 (329)
CUSUM	−3.061/ 6.078	370 (359)	206 (206)	166 (169)	70.9 (65.1)	1158 (1139)
COWL	80.625	370 (370)	358 (359)	381 (380)	369 (370)	370 (370)

Note: Standard deviations are in parentheses.

of the EWMA-CEV method is that W_i is bounded. Thus, the monitoring statistic T_i^U cannot reach control limit L very quickly as the maximum value of W_i is limited. Therefore, we conclude that the COWL chart gives the most satisfactory IC performance.

Tables 2 and 3 present evidence similar to that in Table 1. By comparing Table 2 and Table 3, we can easily deduce the influence of data shape. Similarly, the EWMA-CEV method and the COWL chart demonstrate stable IC performance under various shapes, while the CUSUM chart delivers desirable IC performance only for large β. To be specific, when $\beta = \frac{1}{3}$, the CUSUM chart in Table 3 provides a lighter tailed RL distribution than the geometric distribution, and its notably small FAR value may prevent it from quickly detecting failure as mentioned before. Also, when other values of the parameters η, β, and C are chosen, a similar conclusion about their effects can be drawn.

From Tables 1–3, it can be seen that for each control chart, the control limits under various scenarios are close, and it is necessary to conduct more analysis. Conversely, the control limit L depends not only on the chart, but also on the model parameters such as β and ρ_C. As sometimes there may be uncertainty with (estimated) model parameters, it is necessary to find a more robust control chart. Some sensitivity analyses on the control limit are performed and the results are shown in Table 4. In the simulation, the control limits in Table 1 are selected under the case $\rho_C = 0.7$ and $\beta = 1$ ($\eta = 1$, exponential distribution, we call this case the original scenario hereafter), and the IC ARLs (as well as SDRLs) are computed under four different scenarios with the selected control limits. The simulation results and settings of the four scenarios are shown in Table 4. From the table, we find that Scenario I and II differ from the original scenario only in censoring rate ρ_C, and Scenario III and IV have different shapes from the original setting. In the simulation results, we see that the control limit of the COWL chart is quite robust under different scenarios. For the EWMA-CEV and CUSUM charts, although their control limits are close under various scenarios from previous simulations, they are quite sensitive to model parameters and their IC ARLs deviates distinctly from 370. Another point worth mentioning is that the performance of the EWMA-CEV method is stable regardless of the shape parameter, but it is greatly affected by the censoring rate ρ_{sC}. Thus, it matters little to the COWL chart when either β or ρ_C changes. And the proposed COWL chart has some desirable advantages in terms of its IC performance and robustness.

4.2. Out of Control Performance

In this subsection, the proposed COWL control chart is compared with the two competing methods in terms of the OC performance. The OC comparison focuses on detecting the shifts in the scale parameter, and the settings are similar to those in the IC study. Additional simulations are conducted to illustrate the ability of our proposed method to monitor two parameters simultaneously.

During the OC study, the behavior of each control chart is investigated with various shifts. To assess the overall performance of certain chart, besides the OC ARLs, the relative mean index (RMI) proposed by Han and Tsung [7] is also used. The RMI can be expressed as

Table 5. OC performance when $\beta = 1$ ($\eta_0 = 1$).

	$\rho_C = 0.7$			$\rho_C = 0.4$			$\rho_C = 0.1$		
η	EWMA-CEV	CUSUM	COWL	EWMA-CEV	CUSUM	COWL	EWMA-CEV	CUSUM	COWL
	$\lambda = 0.02$	d=50%	$\lambda = 0.02$	$\lambda = 0.02$	d=50%	$\lambda = 0.02$	$\lambda = 0.05$	d=50%	$\lambda = 0.05$
0.3	21.9 (5.66)	12.6 (5.82)	15.6 (6.98)	27.0 (5.59)	10.4 (3.70)	15.8 (5.54)	19.7 (2.34)	10.3 (3.33)	12.9 (4.48)
0.5	42.6 (16.6)	30.4 (20.6)	32.2 (18.4)	35.1 (9.44)	21.5 (12.7)	26.7 (11.8)	29.3 (6.99)	19.6 (10.7)	21.4 (9.59)
0.7	94.3(53.4)	94.5 (83.8)	80.1 (60.7)	70.3 (31.2)	68.9 (58.5)	58.7 (36.2)	56.9 (25.7)	60.4 (51.4)	51.2 (35.6)
0.9	276 (217)	309 (300)	267 (260)	232 (171)	289 (286)	228 (208)	217 (175)	279 (277)	242 (233)
1	371 (304)	371 (358)	368 (366)	368 (300)	367 (365)	372 (370)	372 (333)	367 (366)	370 (372)
1.1	304 (237)	291 (268)	297 (290)	252 (192)	249 (236)	234 (228)	220 (186)	218 (212)	209 (204)
1.3	158 (100)	148 (118)	141 (120)	106 (60.5)	96.3 (78.9)	85.0 (68.5)	74.6 (49.4)	67.3 (57.8)	65.6 (56.2)
1.5	106 (55.0)	93.6 (64.6)	87.4 (65.8)	67.5 (31.0)	55.2 (38.6)	50.6 (35.1)	43.4 (23.5)	37.0 (26.9)	35.1 (26.0)
1.7	82.6 (36.8)	69.7 (41.8)	64.7 (43.8)	52.3 (20.6)	39.5 (24.2)	36.8 (23.3)	31.6 (14.9)	23.2 (16.2)	24.1 (16.4)
2	65.7 (24.6)	53.0 (27.5)	49.5 (29.8)	40.8 (13.7)	29.0 (15.5)	27.8 (15.8)	23.4 (9.71)	17.7 (10.2)	16.9 (10.3)
RMI	0.259	0.067	0.035	0.443	0.094	0.084	0.299	0.067	0.055

Note: Standard deviations are in parentheses.

Table 6. OC performance when $\beta = \frac{1}{3}$ ($\eta_0 = 0.5$).

	$\rho_C = 0.7$			$\rho_C = 0.4$			$\rho_C = 0.1$		
η	EWMA-CEV	CUSUM	COWL	EWMA-CEV	CUSUM	COWL	EWMA-CEV	CUSUM	COWL
	$\lambda = 0.02$	$d = 50\%$	$\lambda = 0.02$	$\lambda = 0.02$	$d = 50\%$	$\lambda = 0.02$	$\lambda = 0.02$	$d = 50\%$	$\lambda = 0.02$
0.15	82.2 (43.6)	74.7 (45.3)	65.9 (49.3)	62.0 (25.5)	51.6 (27.6)	41.2 (28.8)	56.9 (18.4)	43.8 (20.6)	42.1 (22.8)
0.25	153 (104)	146 (109)	135 (119)	113 (64.7)	103 (72.7)	86.0 (74.2)	98.1 (47.4)	85.9 (57.7)	81.3 (58.1)
0.35	262 (202)	260 (217)	247 (240)	212 (152)	213 (181)	188 (186)	188 (126)	189 (158)	177 (157)
0.45	357 (293)	361 (308)	353 (354)	347 (278)	355 (317)	337 (347)	339 (272)	352 (321)	344 (340)
0.5	370 (304)	372 (315)	373 (374)	367 (302)	373 (330)	369 (378)	370 (304)	373 (341)	374 (374)
0.55	364 (296)	359 (298)	366 (366)	350 (283)	346 (301)	348 (350)	337 (275)	328 (294)	332 (332)
0.65	312 (244)	302 (236)	311 (303)	262 (202)	255 (207)	259 (244)	228 (174)	218 (183)	212 (202)
0.75	259 (193)	248 (184)	256 (242)	197 (141)	187 (140)	190 (170)	157 (110)	148 (113)	141 (126)
0.85	219 (155)	208 (145)	209 (191)	155 (103)	147 (102)	146 (122)	120 (77.8)	112 (78.9)	104 (87.1)
1	176 (116)	170 (109)	165 (144)	120 (72.3)	113 (71.2)	109 (84.4)	90.0 (51.8)	82.3 (53.0)	74.5 (57.9)
RMI	0.074	0.035	0.009	0.137	0.076	0.004	0.133	0.051	0.003

Note: Standard deviations are in parentheses.

$$\text{RMI} = \frac{1}{m}\sum_{i=1}^{m}\frac{\text{ARL}_{\boldsymbol{\theta}_i} - \text{MARL}_{\boldsymbol{\theta}_i}}{\text{MARL}_{\boldsymbol{\theta}_i}}$$

where m is the number of shifts considered, ARL_{θ_i} is the OC ARL of certain control chart when the monitored parameter changes to $\boldsymbol{\theta}_i$, and MARL_{θ_i} is the smallest OC ARL among all the charts needed to detect $\boldsymbol{\theta}_i$. As a matter of fact, the RMI index can be seen as the average percentages deviation of a control chart from the best performing chart. This evaluation index is commonly used when the overall performance of a control chart needs to be assessed. Generally, a control chart with a smaller RMI is considered better. Here, the RMI index is calculated from all the considered shifts shown in the tables except in the IC scenario. Each time a number of IC observations are sampled before the OC shift appears, and thus the process shifts from a steady IC state.

First, we detect the shifts in the scale parameter. The simulation results are shown in Tables 5–7, where cases with different censoring rates and shape parameters are included. As mentioned before, the predetermined shift size $d = 50\%$ in the CUSUM chart, and for fair comparisons, the EWMA smoothing parameter λ in the EWMA-CEV and COWL charts should be appropriately chosen. Particularly, we suggest that λ is selected so that the corresponding chart can reach its best detection at the shift levels $\eta_1 = (1 + d)\eta_0$ or $\eta_2 = (1 - d)\eta_0$, where the CUSUM scheme can perform optimally. For example, in the case of $\rho_C = 0.4$ in Table 5, we find that λs of the EWMA-CEV and COWL charts are close to 0.02 when both charts are performing well at the shift levels $\eta_1 = 1.5$ and $\eta_2 = 0.5$. Similarly, in other scenarios, the tuning parameter λ is given a quick search and listed in the table.

From the result in Table 5, we can see that under whatever censoring rate, the proposed COWL chart gives the smallest OC ARL for almost all shifts except large ones. The differences between the COWL and CUSUM charts are not evident for some large shifts, especially when ρ_C is not high. However, they gradually become noticeable when the shifts

Table 7. OC performance when $\beta = 1.5$ ($\eta_0 = 2$).

	$\rho_C = 0.7$			$\rho_C = 0.4$			$\rho_C = 0.1$		
η	EWMA-CEV	CUSUM	COWL	EWMA-CEV	CUSUM	COWL	EWMA-CEV	CUSUM	COWL
	$\lambda = 0.03$	$d = 50\%$	$\lambda = 0.03$	$\lambda = 0.06$	$d = 50\%$	$\lambda = 0.06$	$\lambda = 0.07$	$d = 50\%$	$\lambda = 0.07$
1	24.0 (7.59)	15.4 (9.43)	16.9 (8.50)	19.1 (4.19)	11.8 (6.01)	13.3 (5.4)	19.7 (3.17)	11.3 (5.31)	13.6 (5.00)
1.4	55.5 (27.3)	57.0 (50.5)	44.0 (30.5)	38.7 (16.7)	41.8 (35.5)	32.5 (21.4)	35.1 (12.2)	38.7 (32.3)	30.0 (17.8)
1.8	218 (172)	278 (276)	205 (196)	174 (142)	260 (259)	189 (180)	151 (117)	254 (255)	190 (180)
2	371 (318)	369 (364)	370 (368)	367 (330)	369 (369)	371 (373)	370 (339)	372 (374)	372 (372)
2.2	253 (198)	249 (232)	256 (245)	197 (164)	201 (194)	198 (192)	159 (134)	169 (166)	148 (143)
2.6	106 (60.5)	99.1 (77.7)	96.5 (76.8)	64.2 (38.5)	60.0 (47.8)	59.5 (48.0)	44.0 (26.1)	41.2 (34.3)	37.5 (30.0)
3	70.1 (31.4)	59.6 (38.9)	58.2 (38.8)	39.5 (18.3)	32.8 (21.7)	32.6 (22.3)	25.8 (12.2)	20.7 (14.4)	19.8 (13.5)
3.4	55.4 (20.8)	44.2 (24.6)	43.7 (25.8)	30.2 (11.8)	23.6 (13.4)	23.3 (14.1)	19.0 (7.87)	14.1 (8.74)	13.8 (8.46)
4	45.2 (13.7)	34.3 (16.2)	34.0 (17.5)	23.7 (7.74)	17.6 (8.61)	17.5 (9.08)	14.4 (5.19)	10.1 (5.44)	9.95 (5.35)
RMI	0.225	0.090	0.016	0.219	0.104	0.027	0.286	0.162	0.058

Note: Standard deviations are in parentheses.

are reduced. The EWMA-CEV method presents acceptable results for some lower-side small shifts, but it lacks efficiency in detecting large shifts in both directions. Thus, the COWL chart outperforms its two competitors, which is also reflected in its small RMI value. Conversely, we find that the censoring rate ρ_C affects OC ARL values as well. As ρ_C decreases and less data become censored, the OC performance of all three charts improve (except for very few cases). In fact, we can expect that the control chart will reach its optimal performance when $\rho_C = 0$ as no information is missing.

The OC performance for Weibull data with other shapes are shown in Tables 6 and 7. We can see that the proposed COWL chart still outperforms the other two methods. To be specific, the performance of the COWL chart is quite satisfactory in Table 6, and its RMI values are much smaller than those of its competitors. In Table 7, the COWL chart presents the best detection capability under most shift levels, and its advantage is less distinct for some upper-side large shifts and the CUSUM chart performs slightly better for some lower-side large shifts. Considering the effect of the data shape, we find that a smaller β leads to a larger OC ARL value while a larger β brings faster detection. This is intuitive as well as the shape of Weibull data is unimodal when $\beta > 1$. However, it becomes more skewed as β decreases which complicates the monitoring procedure. When β falls below 1, the shape of Weibull data degenerates to monotone decreasing (can be seen as the extremely skewed case) so that the OC ARL would be much larger. Combining the results in Tables 5–7, we can conclude that regardless of the value of β, the COWL chart is more appealing than its two alternatives.

Additional simulations are performed to demonstrate the validity of the COWL chart in simultaneous monitoring. The simulation results are shown in Table 8. The IC parameters are selected as $\eta_0 = \beta_0 = 1$. For Weibull data with other shapes, the results are not presented here for simplicity, but the conclusions are similar. For the CUSUM chart, the predetermined shift sizes for two parameters are $d_\eta = 50\%$ and $d_\beta = 20\%$. However, in this simulation, we find that the IC ARL of the CUSUM chart is discrete and cannot reach 370. We thus set the IC ARL to 270 instead.

The simulation results in Table 8 show that the COWL chart still performs robustly under most shift levels. Also, compared with the two competitors, our chart has a much smaller RMI value and consequently a better overall performance. In fact, we find that the large RMI value of the EWMA-CEV method and the CUSUM chart may be caused by their ineffectiveness in detecting certain shifts. In particular, the OC ARLs of the EWMA-CEV and the CUSUM chart are even larger than the fixed IC ARL (270) under several shift levels and this may lead to inefficient detection. However, our chart works reasonably well and is able to detect the shifts in most directions. Thus, the COWL chart is more suitable for practical use than its alternatives.

In the above simulations, the EWMA smoothing parameter λ is selected according to the predetermined shift size d for the CUSUM chart. However, this may not reveal the whole picture of how λ affects the OC performance. A simple simulation to explore the effect of λ is thus performed. In this simulation, we apply the one-parameter monitoring for illustration and test four λ values including 0.02, 0.04, 0.06, and 0.08. The IC parameter $\eta_0 = 1$ (β is fixed at 1) and the log of OC ARL for each λ is plotted in Fig. 1. From the plots, we find that a small λ is more effective for small shifts while a large λ is suitable for large shifts as expected. Furthermore, for lower-side shifts, we see that the differences between various λs are not significant until the shift size grows. Another finding from this λ study is that the censoring rate ρ_C may influence the choice of optimal λ. When ρ_C is large, small λ offers some distinct advantages for upper-side shifts, and the proposed control chart performs quite robustly even when the OC $\eta_1 > 3$. However, this benefit is reduced as ρ_C becomes smaller. Thus, based on $\lambda \in [0.02, 0.1]$ suggested in the

Table 8. OC performance for two parameter monitoring.

		$\rho_C = 0.7$			$\rho_C = 0.4$			$\rho_C = 0.1$		
η	β	EWMA-CEV	CUSUM	COWL	EWMA-CEV	CUSUM	COWL	EWMA-CEV	CUSUM	COWL
		$\lambda = 0.05$		$\lambda = 0.05$	$\lambda = 0.06$		$\lambda = 0.06$	$\lambda = 0.06$		$\lambda = 0.06$
0.2	0.6	13.5 (3.73)	7.64 (5.68)	7.54 (4.40)	15.6 (3.44)	7.87 (5.44)	7.77 (4.12)	17.6 (3.51)	7.63 (4.99)	8.28 (4.20)
	0.8	13.0 (3.24)	8.73 (6.46)	8.49 (4.40)	13.8 (2.22)	8.56 (5.34)	8.85 (3.98)	15.8 (1.80)	7.95 (4.44)	9.20 (3.98)
	1	12.4 (2.80)	9.72 (7.06)	8.57 (4.29)	12.9 (1.52)	8.98 (5.14)	9.30 (3.56)	15.2 (1.12)	8.35 (4.17)	9.70 (3.85)
	1.2	11.8 (2.41)	10.5 (7.64)	8.31 (3.88)	12.5 (1.12)	9.44 (5.00)	9.37 (3.39)	15.0 (0.75)	8.70 (4.01)	10.0 (3.63)
	1.4	11.3 (2.11)	11.3 (7.67)	7.84 (3.60)	12.3 (0.89)	10.0 (4.93)	9.44 (3.25)	15.0 (0.50)	9.06 (3.92)	10.3 (3.65)
0.6	0.6	29.4 (13.4)	25.9 (23.8)	15.9 (11.8)	40.0 (20.5)	25.6 (20.6)	17.4 (12.2)	59.1 (37.3)	24.9 (21.8)	16.8 (11.5)
	0.8	38.0 (19.1)	54.7 (47.0)	28.6 (22.5)	38.8 (18.8)	37.1 (23.1)	30.1 (22.4)	42.6 (20.3)	32.8 (23.4)	30.9 (22.2)
	1	50.8 (29.1)	106 (69.5)	44.8 (39.4)	37.4 (16.8)	42.4 (20.0)	35.3 (25.5)	34.7 (12.2)	30.1 (15.2)	34.1 (21.7)
	1.2	72.8 (47.5)	169 (83.2)	59.0 (56.1)	35.8 (14.9)	42.6 (16.4)	30.2 (20.6)	31.0 (8.29)	26.4 (9.86)	27.4 (14.0)
	1.4	113 (84.3)	236 (96.8)	60.8 (58.4)	33.8 (12.8)	41.1 (13.8)	23.0 (14.7)	29.4 (6.38)	24.5 (7.48)	22.2 (9.77)
0.8	0.6	41.2 (21.9)	38.5 (36.0)	21.2 (17.4)	69.6 (46.3)	38.6 (33.0)	23.2 (18.0)	115 (91.5)	35.7 (33.4)	19.7 (14.1)
	0.8	67.9 (43.6)	95.0 (77.2)	48.8 (43.7)	84.5 (58.8)	71.7 (53.4)	58.8 (51.4)	109 (81.2)	75.3 (68.5)	55.6 (48.7)
	1	135 (106)	200 (127)	126 (129)	101 (72.8)	100 (65.8)	115 (110)	86.4 (55.8)	86.2 (68.7)	112 (107)
	1.2	269 (234)	319 (195)	185 (201)	119 (88.6)	118 (72.2)	88.7 (82.8)	70.2 (37.0)	65.9 (41.8)	58.8 (47.0)
	1.4	225 (186)	314 (212)	126 (124)	139 (106)	129 (77.8)	50.6 (43.0)	61.9 (27.0)	53.1 (27.3)	31.9 (19.5)
1	0.6	57.8 (35.7)	50.3 (47.1)	26.6 (22.6)	127 (100)	52.3 (48.2)	26.9 (21.3)	104 (82.8)	39.8 (37.4)	20.3 (14.0)
	0.8	130 (101)	139 (112)	86.2 (86.2)	200 (171)	133 (121)	88.6 (84.5)	163 (138)	110 (108)	63.5 (56.7)
	1	273 (240)	273 (204)	272 (301)	269 (238)	275 (227)	273 (285)	268 (236)	272 (233)	268 (281)
	1.2	157 (122)	236 (184)	183 (193)	272 (239)	375 (251)	152 (157)	404 (367)	389 (267)	111 (106)
	1.4	83.7 (50.8)	145 (127)	84.5 (76.2)	221 (187)	388 (234)	71.2 (63.5)	478 (430)	388 (250)	42.1 (34.3)
1.2	0.6	80.5 (55.6)	65.3 (61.9)	32.0 (27.5)	191 (163)	66.6 (63.8)	30.6 (24.6)	65.9 (48.2)	36.6 (35.0)	19.4 (13.5)
	0.8	227 (193)	185 (156)	124 (125)	196 (165)	166 (157)	95.6 (91.3)	79.8 (59.9)	87.4 (85.4)	47.5 (40.7)
	1	178 (140)	225 (185)	242 (253)	132 (104)	225 (194)	158 (161)	99.7 (76.4)	200 (178)	108 (109)
	1.2	83.6 (51.0)	141 (126)	102 (95.8)	88.4 (61.2)	201 (169)	87.0 (82.2)	132 (105)	360 (226)	77.7 (72.7)
	1.4	53.5 (25.3)	82.5 (74.8)	54.2 (41.4)	65.2 (39.6)	164 (143)	49.0 (38.8)	188 (154)	468 (187)	40.0 (32.2)
1.4	0.6	113 (86.5)	79.7 (75.9)	37.6 (34.2)	182 (153)	74.4 (71.9)	31.9 (25.5)	46.3 (30.7)	31.8 (30.0)	18.1 (12.2)
	0.8	253 (218)	199 (176)	147 (151)	112 (86.1)	142 (138)	77.6 (71.2)	47.1 (30.1)	59.2 (56.9)	34.4 (28.0)
	1	108 (74.6)	166 (145)	150 (148)	68.9 (44.2)	135 (128)	79.0 (71.1)	48.7 (29.8)	99.8 (96.9)	48.9 (43.5)
	1.2	59.2 (29.6)	90.6 (82.6)	66.7 (54.7)	48.9 (26.8)	100 (95.2)	48.5 (38.8)	50.8 (30.1)	160 (142)	41.1 (33.7)
	1.4	42.3 (16.4)	54.2 (46.5)	41.4 (27.9)	38.7 (18.2)	74.5 (70.1)	33.1 (23.5)	53.9 (31.4)	239 (172)	29.4 (21.3)
1.8	0.6	201 (170)	104 (99.3)	47.0 (43.8)	101 (75.8)	74.3 (71.6)	31.0 (24.3)	30.0 (16.9)	23.5 (21.0)	15.3 (9.98)
	0.8	140 (104)	170 (151)	134 (132)	54.9 (32.8)	81.3 (77.5)	47.7 (38.9)	27.1 (14.0)	31.2 (28.2)	20.7 (15.3)
	1	62.7 (33.0)	94.1 (86.3)	74.1 (64.4)	37.4 (17.9)	58.2 (53.4)	37.6 (28.3)	25.2 (11.9)	36.8 (33.6)	21.5 (15.9)
	1.2	41.8 (16.2)	52.8 (45.0)	42.1 (29.6)	29.1 (11.7)	40.2 (35.3)	26.3 (17.5)	23.8 (10.6)	41.4 (38.5)	19.5 (13.4)
	1.4	33.1 (10.1)	34.8 (28.2)	30.5 (17.8)	24.4 (8.58)	29.8 (24.9)	20.6 (11.9)	22.8 (9.48)	49.2 (46.1)	16.8 (10.4)
RMI		0.525	0.709	0.043	0.943	0.813	0.017	1.404	1.569	0.037

Note: Standard deviations are in parentheses.

guideline, the optimal λ really depends on the censoring rate, shift directions and other model parameters.

To summarize, our COWL chart not only performs well in detecting scale shifts, but is also robust in two parameter monitoring. Our simulation is conducted under various censoring rates and data shapes, and the advantage of the COWL chart is noticeable. Combined with its robust IC performance, the COWL chart is indeed a useful tool for monitoring censored lifetime data.

4.3. OC Performance Study of Self-Starting Chart

In previous simulation studies, the model parameter η_0 is estimated from sufficient IC samples. However, this may not always be achieved in reality. In this subsection, we investigate the OC performance of the self-starting version of our control chart (SS-COWL). As there is no self-starting strategy in the EWMA-CEV method and the CUSUM chart, we only present the result of our SS-COWL chart for illustration.

Following the previous OC performance studies, cases with different censoring rates are considered in the simulation. The shape parameter $\beta_0 = 1$ for simplicity (exponential distribution), and the EWMA smoothing coefficient λ is selected to be 0.05 in all cases for consistency. As mentioned in the literature (Hawkins et al. [10], Zou and Tsung [35]), the OC performance of the self-starting chart is affected by the location of the change point τ. We include several scenarios with different change point times $\tau = 30, 60$, and 100 in the simulation while the number of historical IC samples

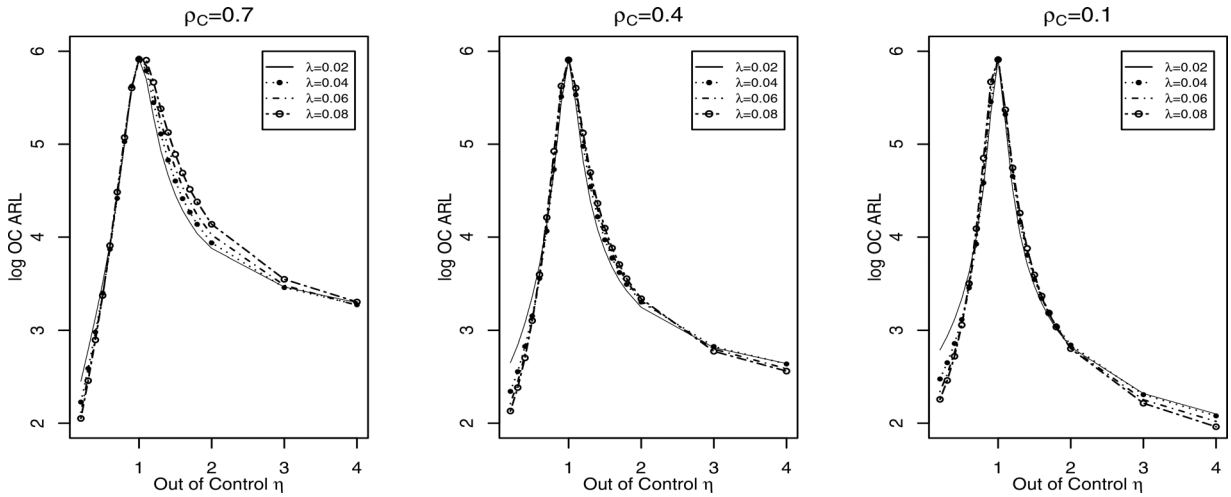

Figure 1. The OC performances of our method are shown under different censoring rates when various values of λ are selected.

Table 9. Performance of self-starting chart when $\eta_0 = 1$.

	$\rho_C = 0.7$			$\rho_C = 0.4$			$\rho_C = 0.1$		
η_1	$\tau = 30$	$\tau = 60$	$\tau = 100$	$\tau = 30$	$\tau = 60$	$\tau = 100$	$\tau = 30$	$\tau = 60$	$\tau = 100$
0.3	55.3	22.0	20.8	29.8	17.5	17.6	26.0	17.5	16.5
0.5	210	95.6	60.7	136	51.3	39.3	88.6	38.6	33.5
0.7	313	238	181	290	194	135	258	158	108
0.9	352	316	283	345	310	276	340	298	265
1.1	360	328	299	342	308	275	327	282	248
1.3	357	310	284	310	244	194	275	194	143
1.5	346	276	245	271	180	124	216	113	74.7
1.7	333	245	218	230	125	82.3	162	65.8	45.9
2	313	198	132	177	77.2	52.0	101	35.6	30.3
3	259	110	66.7	79.2	31.0	27.8	32.2	15.8	17.0
4	235	77.4	50.4	48.3	22.3	22.3	20.3	11.8	13.0

is fixed at 10. The OC ARL values of the SS-COWL chart are shown in Table 9. From the results, it can be seen that a larger τ gives a better OC performance for all shifts, which is quite understandable as the updated parameter becomes more accurate when more IC observations are collected. Particularly, a moderate τ would give a stable OC ARL for detecting large shifts (the value of $\tau = 60$ is appropriate when $\eta_1 = 0.3$) while a larger τ is required for detecting small shifts. Conversely, from the simulation, we see that the censoring rate ρ_C may influence the performance of the SS-COWL chart as well. From the previous simulation results, we know that a greater censoring rate ρ_C may lead to a larger OC ARL, and a similar conclusion can be drawn here. Moreover, a larger τ may be needed for a large ρ_C and it decreases as ρ_C becomes smaller. Finally, comparing the results in Table 9 and Table 5 for the case $\rho_C = 0.1$, we note that the self-starting chart cannot perform as well as the nonself-starting chart even when τ is large enough. However, the self-starting chart is still a useful tool when there are insufficient historical data.

5. A REAL EXAMPLE

In this section, we apply the proposed method to a real dataset on the breaking strength of carbon fibers. Carbon fiber is a very important industrial material and is used to reinforce composite materials. Under increasing stress (unit, Gpa), carbon fibers may break into pieces and thus it is important to monitor the manufacturing and testing procedures, which is also a typical lifetime/failure application. The dataset has also been studied by Guo and Wang [6] and Pascual and Li [21].

Figure 2 plots the 100 observations in the dataset, of which half are IC observations and the other half are OC observations. The IC observations are assumed to follow the Weibull distribution, and the IC parameters are estimated to be $\eta = 3.2 \text{and} \beta = 4.8$ by MLE. To confirm the assumption, the Kolmogorov-Smirnov (KS) test is performed (using the test function in R) on the IC observations and the obtained *P*-value is 0.39, validating the assumption. As the provided data are real raw data, we need to perform censoring. We fix

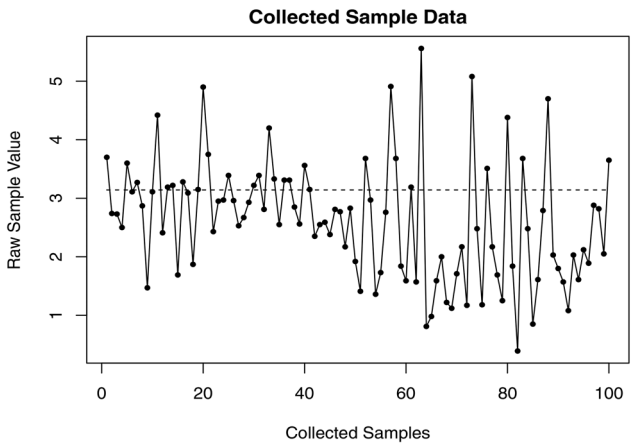

Figure 2. Sample data from the carbon fiber application. The first 50 observations are IC observations and the last 50 are OC observations. The dashed horizontal line indicates the censoring threshold.

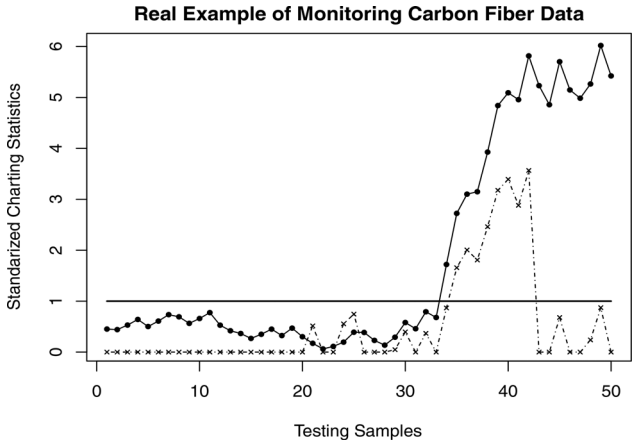

Figure 3. Monitoring carbon fiber data with both the COWL chart and the CUSUM chart. The solid horizontal line represents the common standardized control limit $y = 1$.

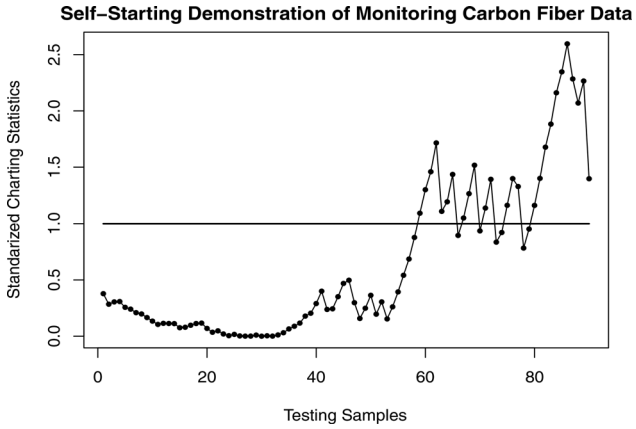

Figure 4. Self-starting demonstration of monitoring carbon fiber data. The solid horizontal line represents the standardized control limit $y = 1$.

the censoring rate $\rho_C = 0.4$ and the corresponding censoring threshold $C = 3.14$. The dashed line in Fig. 2 represents the censoring threshold. For both IC and OC observations, the real value is censored when it is larger than 3.14, and the corresponding observed value can only be 3.14.

For online monitoring, as the carbon fiber data are based on single observation, the CUSUM chart in Dickinson et al. [5] is selected for comparison. The settings are the same with those in the simulation studies, and the EWMA parameter λ is fixed at 0.05. Online steady-state monitoring is applied in this example. Twenty IC samples are monitored first, followed by 30 OC samples. The monitoring results are summarized in Fig. 3. To present the results more straightforwardly, the monitoring statistics in Fig. 3 are transformed into the standardized charting statistics (i.e., monitoring statistics divide the control limit). Thus, both the COWL and the CUSUM methods have the same new control limit (equals to 1), and it is plotted with the solid horizontal line. In the figure, the change point is at the 20th sample and we see the proposed COWL chart takes 14 OC samples to signal while the CUSUM chart takes 15. Therefore, our control chart performs slightly better than the CUSUM method in terms of the OC performance. More interestingly, while the charting statistic of CUSUM method returns to the IC region as more OC samples are collected, the COWL chart keeps signaling after the change point. Thus, the robustness of the COWL chart is proven.

Besides the traditional monitoring case, the self-starting scenario is also considered in this real data example. As no other methods applies the self-starting strategy, we only plot the result of our SS-COWL chart for demonstration here. The parameter τ in this self-starting case study equals to 40, and 30 OC samples (same OC samples with nonself-starting case study) are picked for testing. The monitoring results are shown in Fig. 4. From the figure, it is clear to see that the change point occurs at 40th point, and our SS-COWL chart takes 21 steps to signal.

6. CONCLUSIONS AND FUTURE WORK

This article proposes a novel method for monitoring Weibull-distributed lifetimes, and derives a new control chart by employing the newly developed EWMA strategy for likelihood. The proposed COWL chart focuses on detecting changes in the scale parameter, and can handle the censoring phenomenon reasonably well. Compared with competing methods, our proposed method not only provides satisfying IC and OC performance, but is also robust to various scenarios. The method focuses on single observation monitoring,

and it is easy to implement. The self-starting version of the control chart is also introduced for use when the number of reference samples is insufficient. The superiority of our method has been proven through numerical simulations and a real data example.

However, there are a number of outstanding issues. The first one is Phase I analysis. Although the COWL chart is robust and a self-starting control chart has been proposed, a "clean" IC dataset is still essential before online monitoring. Outliers must be removed from the historical dataset using the clustering methods or change-point models. Furthermore, as the number of Phase I samples may affect the performance of the control chart (nonself-starting chart), it is necessary to work out how large the sample size should be to ensure robust parameter estimation. Finally, most lifetime/failure process observations are assumed to come from the parametric families, but this is not always true (Li and Kong [17]). It will be of great interest to extend the current monitoring problem to the nonparametric framework where the censoring phenomenon still exists. As the distribution density is unknown under the nonparametric scenario, the likelihood method may not be directly applicable and more general monitoring strategies are called for.

APPENDIX: ASYMPTOTIC PROPERTIES OF THE WEIGHTED LRT STATISTIC

Assuming the observed data follows Weibull distribution with scale parameter η and shape parameter β, thus, for data x, its probability density function becomes

$$f(x;\eta,\beta)=\frac{\beta}{\eta}\left(\frac{x}{\eta}\right)^{\beta-1}\exp^{-\left(\frac{x}{\eta}\right)^{\beta}} \tag{11}$$

When data are censored (right censoring) with censoring threshold C, then the observed data y becomes

$$y\sim\begin{cases}x & x\le C\\ C & \text{otherwise}\end{cases} \tag{12}$$

and the indicator function $\delta(x)$ equals

$$\delta\sim\begin{cases}1 & x\le C\\ 0 & \text{otherwise}\end{cases} \tag{13}$$

Then, for the observed data y_j, its observed log-likelihood is

$$l(y_j;\eta,\beta)=\delta_j\left[-\beta\log\eta+\log\beta+(\beta-1)\log y_j-\left(\frac{y_j}{\eta}\right)^{\beta}\right]-(1-\delta_j)\left(\frac{C}{\eta}\right)^{\beta} \tag{14}$$

In the following, we derive the asymptotic properties of the weighted LRT statistics (the monitoring statistic of the COWL chart). By employing the EWMA technique, the likelihood of each observations is assigned with different weight. Thus, the weighted the loglikelihood of observations $\boldsymbol{y}$ is

$$\begin{aligned}l(\boldsymbol{y};\eta,\beta)&=\Sigma_{j=1}^{n}\omega_{j,\lambda}l(y_j,\eta,\beta)\\&=\Sigma_{j=1}^{n}\omega_{j,\lambda}\left(\delta_j\left[-\beta\log\eta+\log\beta+(\beta-1)\log y_j-\left(\frac{y_j}{\eta}\right)^{\beta}\right]\right)\\&\quad-\Sigma_{j=1}^{n}\omega_{j,\lambda}(1-\delta_j)\left(\frac{C}{\eta}\right)^{\beta}\end{aligned} \tag{15}$$

where $\omega_{j,\lambda}$ is the EWMA weight. Then, in single-parameter monitoring, the maximum-weighted likelihood estimate (WMLE) of the scale parameter η is derived as

$$\begin{aligned}\hat{\eta}_t&=\underset{\eta}{\operatorname{argmax}}L(\eta;\boldsymbol{y},\beta_0)\\&=\left(\frac{\Sigma_{j=1}^{n}\omega_{j,\lambda}[\delta_j y_j^{\beta_0}+(1-\delta_j)C^{\beta_0}]}{\Sigma_{j=1}^{n}\omega_{j,\lambda}\delta_j}\right)^{\frac{1}{\beta_0}}\end{aligned} \tag{16}$$

Then, the monitoring statistics of the weighted LRT is

$$\begin{aligned}T_{\{\eta\},n}&=l(\hat{\eta};\boldsymbol{y},\beta_0)-l(\eta_0;\boldsymbol{y},\beta_0)\\&=\Sigma_{j=1}^{n}\omega_{j,\lambda}\delta_j\left[\beta_0\log\frac{\eta_0}{\hat{\eta}}+\left(\frac{y_j}{\eta_0}\right)^{\beta_0}-\left(\frac{y_j}{\hat{\eta}}\right)^{\beta_0}\right]\\&\quad+\Sigma_{j=1}^{n}\omega_{j,\lambda}(1-\delta_j)\left[\left(\frac{C}{\eta_0}\right)^{\beta_0}-\left(\frac{C}{\hat{\eta}}\right)^{\beta_0}\right]\\&=\Sigma_{j=1}^{n}\omega_{j,\lambda}\delta_j\left[\log(\frac{\eta_0}{\hat{\eta}}^{\beta_0})\right]+\Sigma_{j=1}n\omega_{j,\lambda}(1-\delta_j)\left(\frac{C}{\eta_0}\right)^{\beta_0}\\&\quad-\frac{\Sigma_{j=1}^{n}\omega_{j,\lambda}\left[\delta_j y_j^{\beta_0}+(1-\delta_j)C^{\beta_0}\right]}{\hat{\eta}^{\beta_0}}\\&=\Sigma_{j=1}^{n}\omega_{j,\lambda}\delta_j\log\frac{\Sigma_{j=1}^{n}\omega_{j,\lambda}\delta_j}{\Sigma_{j=1}^{n}\omega_{j,\lambda}\left[\delta_j\left(\frac{y_j}{\eta_0}\right)^{\beta_0}+(1-\delta_j)\left(\frac{C}{\eta_0}\right)^{\beta_0}\right]}\\&\quad-\Sigma_{j=1}^{n}\omega_{j,\lambda}\delta_j+\Sigma_{j=1}^{n}\omega_{j,\lambda}\left[\delta_j\left(\frac{y_j}{\eta_0}\right)^{\beta_0}+(1-\delta_j)\left(\frac{C}{\eta_0}\right)^{\beta_0}\right]\end{aligned} \tag{17}$$

For $X\sim\text{Weibull}(\eta_0,\beta_0)$, then $\left(\frac{X}{\eta_0}\right)^{\beta_0}\sim\exp(1)$. Thus, $\left(\frac{y_j}{\eta_0}\right)^{\beta_0}$ follows the standard exponential distribution with censoring threshold equals to $\left(\frac{C}{\eta_0}\right)^{\beta_0}$. Assume $Q=\Sigma_{j=1}^{n}\omega_{j,\lambda}\delta_j$, $Z=\Sigma_{j=1}^{n}\omega_{j,\lambda}[\delta_j\left(\frac{y_j}{\eta_0}\right)^{\beta_0}+(1-\delta_j)\left(\frac{C}{\eta_0}\right)^{\beta_0}]$, thus

$$T_{\{\eta\},n}=Q\log Q-Q\log Z-Q+Z \tag{18}$$

We assume $E(Q)=Q_0$, $\text{Var}(Q)=\Sigma_{j=1}^{n}\omega_{j,\lambda}^2\text{Var}(\delta_j)$, and $\text{Var}(\delta_j)$ is fixed and determined by censored rate. As $\omega_{j,\lambda}=\lambda(1-\lambda)^{n-j}$, we have

$$\max_{1\le j\le n}\frac{\omega_{j,\lambda}^2}{\Sigma_{j=1}^{n}\omega_{j,\lambda}^2}=\frac{\lambda^2}{\lambda^2(1+(1-\lambda)^2+(1-\lambda)^4+\dots)}\to 0 \tag{19}$$

as $\lambda n\to\infty$ and $\lambda\to 0$. Thus, according to Hajek-Sidak's theorem, we have

$$[\text{Var}(Q)]^{-\frac{1}{2}}(Q-Q_0)\to^{d}N(0,1) \tag{20}$$

Similarly, for Z, we have

$$[\mathrm{Var}(Z)]^{-\frac{1}{2}}(Z - Z_0) \to^d N(0,1)$$

Noting $Q \to^p Q_0$ and $Z \to^p Z_0$, we do second-order Taylor-expansion to $Q \log Q$ and $\log Z$. Then we have

$$\begin{aligned} T_{\{\eta\},n} &= Q_0 \log Q_0 + (1 + \log Q_0)(Q - Q_0) \\ &\quad + \frac{1}{2!Q_0}(Q - Q_0)^2 + o((Q - Q_0)^2) \\ &\quad - (Q - Q_0 + Q_0)\Big[\log Z_0 + \frac{1}{Z_0}(Z - Z_0) \\ &\quad - \frac{1}{2!Z_0^2}(Z - Z_0)^2 + o((Z - Z_0)^2)\Big] - Q + Z \end{aligned} \tag{21}$$

By simple calculation, we know $Q_0 = Z_0 = 1 - e^{(-\frac{C}{\eta_0})^{\beta_0}}$, then

$$\begin{aligned} T_{\{\eta\},n} &= Q_0 \log Q_0 + (Q - Q_0) + (Q - Q_0)\log Q_0 \\ &\quad + \frac{1}{2!Q_0}(Q - Q_0)^2 + o((Q - Q_0)^2) \\ &\quad - (Q - Q_0)\log Z_0 - Q_0 \log Z_0 - \frac{Q}{Z_0}(Z - Z_0) \\ &\quad + \frac{Q}{2!Z_0^2}(Z - Z_0)^2 + o((Z - Z_0)^2) - Q + Z \\ &= Z - Q_0 + \frac{1}{2!Q_0}(Q - Q_0)^2 - \frac{Q}{Z_0}(Z - Z_0) \\ &\quad + \frac{Q}{2!Z_0^2}(Z - Z_0)^2 + o((Q - Q_0)^2) + o((Z - Z_0)^2) \\ &= \frac{1}{2!Q_0}(Q - Q_0)^2 - \frac{(Q - Q_0)(Z - Z_0)}{Z_0} \\ &\quad + \frac{Q}{2!Z_0^2}(Z - Z_0)^2 + o((Q - Q_0)^2) + o((Z - Z_0)^2) \\ &= \frac{1}{2Q_0}(Q + Z - Q_0 - Z_0)^2 + o((Q - Q_0)^2) \\ &\quad + o((Z - Z_0)^2) + \frac{1}{2!Z_0^2}o((Q - Q_0)(Z - Z_0)^2) \end{aligned} \tag{22}$$

For $Q + Z$, we can find the $\mathrm{Var}(Q + Z) = \sum_{j=1}^{n} \omega_{j,\lambda}^2 (1 - 4\left(\frac{C}{\eta_0}\right)^{\beta_0} e^{\left(\frac{C}{\eta_0}\right)^{\beta_0}} + 3e^{\left(\frac{C}{\eta_0}\right)^{\beta_0}} - 4e^{2\left(\frac{C}{\eta_0}\right)^{\beta_0}})$, thus we know

$$\frac{2Q_0}{\mathrm{Var}(Q + Z)} T_{\{\eta\},n} \to^d \chi^2(1)$$

that is

$$\frac{2 * (1 - e^{\left(\frac{C}{\eta_0}\right)^{\beta_0}})}{\sum_{j=1}^{n} \omega_{j,\lambda}^2 (1 - 4\left(\frac{C}{\eta_0}\right)^{\beta_0} e^{\left(\frac{C}{\eta_0}\right)^{\beta_0}} + 3e^{\left(\frac{C}{\eta_0}\right)^{\beta_0}} - 4e^{2\left(\frac{C}{\eta_0}\right)^{\beta_0}})} T_{\{\eta\},n} \to^d \chi^2(1)$$

Then, in Proposition 1, we see

$$A = 2 * (1 - e^{\left(\frac{C}{\eta_0}\right)^{\beta_0}})$$

$$B = 1 - 4\left(\frac{C}{\eta_0}\right)^{\beta_0} e^{\left(\frac{C}{\eta_0}\right)^{\beta_0}} + 3e^{\left(\frac{C}{\eta_0}\right)^{\beta_0}} - 4e^{2\left(\frac{C}{\eta_0}\right)^{\beta_0}}$$

ACKNOWLEDGMENTS

The authors thank the Editor, the Associate Editor and two referees for many constructive comments and suggestions, which have greatly improved the quality of the article. This work was supported by National Science Fund of China (No.11501209, No.11271135, No.11571113, No.71402133 and No.71602155), the Postdoctoral Science Foundation of China (2015M570348), Shanghai Rising Star Program (16QA1401700), the Fundamental Research Funds for the Central Universities and the 111 Project (B14019), The International Postdoctoral Exchange Fellowship Program (No. 20160089), RGC General Research Fund 619913 and the Project of Shanghai Universities to enhance the competition and innovation "collaborative innovation of modern statistical methods and theory".

REFERENCES

[1] C. Agostinelli and M. Markatou, Test of hypotheses based on the weighted likelihood methodology, Stat Sin 11 (2001), 499–514.
[2] M. Aslam, A mixed EWMACUSUM control chart for Weibull-distributed quality characteristics. Qual Reliab Eng Int 32 (2016), 2987–2994.
[3] R.G. Baston, Y. Jeong, D.J. Fonseca, and P.S. Ray, Control charts for monitoring field failure data, Qual Reliab Eng Int 22 (2006), 733–755.
[4] Y. Chan, B. Han, and F. Pascual, Monitoring the Weibull shape parameter with type II censored data. Qual Reliab Eng Int, 31 (2016), 741–760.
[5] R.M. Dickinson, D.A. Olteanu, A.R. Driscoll, W.H. Woodall, and G.G. Vining, CUSUM charts for monitoring the characteristic life of censored Weibull lifetimes, J Qual Technol 46 (2014), 340–358.
[6] B. Guo and B.X. Wang, Control charts for monitoring the Weibull shape parameter based on type-II censored sample, Qual Reliab Eng Int 30 (2014), 13–24.
[7] D. Han and F. Tsung, A reference-free cuscore chart for dynamic mean change detection and a unified framework for charting performance comparison, J Am Stat Assoc 101 (2006), 368–386.
[8] D.M. Hawkins, Self-starting CUSUM charts for location and scale, Statistician 36 (1987), 299–316.
[9] D. M. Hawkins and D.H. Olwell, Cumulative sum charts and charting for quality improvement, Springer-Verlag, New York, NY, 1998.
[10] D.M. Hawkins, P. Qiu, and C.W. Kang, The change point model for statistical process control, J Qual Technol 35 (2003), 355–366.
[11] W.A. Jensen, L.A. Jones, C.W. Champ, and W.H. Woodall, Effects of parameter estimation on control chart properties: A literature review, J Qual Technol 38 (2006), 349–364.
[12] L.A. Jones, C.W. Champ, and S.E. Rigdon, The performance of exponentially weighted moving average charts with estimated parameters, Technometrics 43 (2002), 156–167.
[13] J.P. Joseph and R.S. Thomas, Estimation of the change point of a normal mean in SPC application, J Qual Technol 33 (2001), 82–95.
[14] B.C. Khoo and M. Xie, A study of time-between-events control chart for the monitoring of regularly maintained systems, Qual Reliab Eng Int 25 (2009), 805–819.
[15] J.K. Kim and J. Shao, Statistical methods for handling incomplete data, 1st ed., Chapman Hall/CRC, New York, NY, 2013.

[16] J.F. Lawless, Statistical models and methods for lifetime data, 1st ed., John Wiley & Sons, New York, NY, 2003.
[17] Z. Li and Z. Kong, A generalized procedure for monitoring rightcensored failure time data, Qual Reliab Eng Int 31 (2015), 695–705.
[18] W.Q. Meeker and L.A. Escobar, Statistical methods for reliability data, John Wiley & Sons, New York, NY, 1998.
[19] Y. Mei, Is average run length to false alarm always an informative criterionĨ¿, (with discussions), Seq Anal 27 (2008), 354–419.
[20] D.A. Olteanu, Cumulative sum control charts for censored reliability data, Ph.D Thesis, Virginia Polytechnic Institute and State University.
[21] F. Pascual and S. Li, Monitoring the Weibull shape parameter by control charts for the sample range of type II censored data, Qual Reliab Eng Int 28 (2012), 233–246.
[22] P. Qiu, C. Zou, and Z. Wang, Nonparametric profile monitoring by mixed modeling, Technometrics 52 (2010), 265–277.
[23] P. Qiu and C. Zou, Control chart for monitoring nonparametric profiles with arbitrary design, Stat Sin 20 (2010), 1655–1682.
[24] S.M.M. Raza and A.F. Siddiqi, EWMA and DEWMA control charts for Poisson exponential distribution: Conditional median approach for censored data, Qual Reliab Eng Int 32 (2016), doi: 10.1002/qre.2015.
[25] M.S. Shafae, R.M. Dickinson, W.H. Woodall, and J.A. Camelio, Cumulative sum control charts for monitoring Weibull-distributed time between events. Qual Reliab Eng Int 31 (2015), 839–849.
[26] X. Shen, C. Zou, W. Jiang, and F. Tsung, Monitoring Poisson count data with probability control limits when sample sizes are time varying, Nav Res Logist 60 (2013), 625–636.
[27] S.H. Steiner and J. Mackay, Monitoring process with highly censored data, J Qual Technol 32 (2000), 199–208.
[28] S.H. Steiner and J. Mackay, "Detecting changes in the mean from censored lifetime data," in: H.J. Lenz and P.T. Wilrich (Editors), Frontiers in statistical quality control, Phsica-Verlag, 2001, pp. 275-289.
[29] Z.G. Stoumbos and J.H. Sullivan, Robustness to non-normality of the multivariate EWMA control chart, J Qual Technol 34 (2002), 260–276.
[30] P.A. Tobias and D.C. Trindade, Applied reliability, 3rd ed., Chapman Hall/CRC, New York, NY, 2012.
[31] W.H. Woodall and D.C. Montgomery, Some current directions in the theory and application of statistical process monitoring, J Qual Technol 46 (2014), 79–94.
[32] Tuncel M. Yegulalp, Control charts for exponentially distributed product life, Nav Res Logist 22 (1975), 697–712.
[33] L. Zhang and G. Chen, EWMA charts for monitoring the mean of censored Weibull lifetimes, J Qual Technol 36 (2004), 321–328.
[34] Q. Zhou, C. Zou, Z. Wang, and W. Jiang, Likelihood-based EWMA charts for monitoring Poisson count data with time-varying sample size, J Am Stat Assoc 107 (2012), 1049–1062.
[35] C. Zou and F. Tsung, A self-starting control chart for linear profiles, J Qual Technol 39 (2011), 364–375.
[36] C. Zou and F. Tsung, A multivariate sign EWMA control chart, Technometrics 53 (2011), 84–97.